

The significance of trends in long-term correlated records

Araik Tamazian

Institut für Theoretische Physik, Justus-Liebig-Universität Giessen, 35392 Giessen, Germany

Josef Ludescher and Armin Bunde

Institut für Theoretische Physik, Justus-Liebig-Universität Giessen, D-35392 Giessen, Germany

We study the distribution $P(x; \alpha, L)$ of the relative trend x in long-term correlated records of length L that are characterized by a Hurst-exponent α between 0.5 and 1.5 obtained by DFA2. The relative trend x is the ratio between the strength of the trend Δ in the record measured by linear regression, and the standard deviation σ around the regression line. We consider L between 400 and 2200, which is the typical length scale of monthly local and annual reconstructed global climate records. Extending previous work by Lennartz and Bunde [1] we show explicitly that P follows the student-t distribution $P \propto [1 + (x/a)^2/l]^{-(l+1)/2}$, where the scaling parameter a depends on both L and α , while the effective length l depends, for α below 1.15, only on the record length L . From P we can derive an analytical expression for the trend significance $S(x; \alpha, L) = \int_{-x}^x P(x'; \alpha, L) dx'$ and the border lines of the 95% percent significance interval. We show that the results are nearly independent of the distribution of the data in the record, holding for Gaussian data as well as for highly skewed non-Gaussian data. For an application, we use our methodology to estimate the significance of Central West Antarctic warming. PACS numbers: 05.10.-a, 05.45.Tp, 92.70.Mn

I. INTRODUCTION

The variability of a data set $\{y_i\}, i = 1, \dots, L$, depends on its (internal) correlation properties and can be influenced by external mechanisms. Prominent examples are temperature records [1–28], river flows [29–36], and sea level heights [37–39] that all show a strong natural long-term persistence and, in addition, are effected by anthropogenic influences that may lead to an additional trend.

In long-term persistent records, small events have a tendency to cluster in "valleys" while large events tend to cluster in "mountains". Accordingly, long-term persistent records exhibit a pronounced valley-mountain structure, where it is difficult to distinguish a natural trend (starting in a valley and ending in a mountain) from a small external deterministic trend. The problem of estimating the anthropogenic trend in temperature records, river flows and sea level height is an important issue in hydroclimatology and is called the "detection problem" [3, 40–42]. The central quantity here is the probability $P(x; \alpha, L)$ that in a long-term persistent record of length L , characterized by the Hurst exponent α , a relative trend of strength x occurs; x is obtained from the standard linear regression analysis of the record and represents the height Δ of the regression line divided by the standard deviation of y_i around the regression line (see Section II). From P one obtains the significance of the trend as well as its error bars (denoting the 95% significance interval) [1, 3, 22].

In many previous attempts to solve this problem (see, e.g., [43–47, 49]) it had been *tacitly assumed* that the persistence of the climate records can be modelled by an auto-regressive process of first order (AR(1)) which allowed, in a simple and straightforward way, to estimate

the significance of the warming trend Δ and its error bars. In this case, the central quantity is the probability $P(x; C(1), L)$ that in an AR(1) record of length L , characterized by the detrended lag-1 autocorrelation $C(1)$, a relative trend of strength x occurs. It is well known that $P(x; C(1), L)$ follows a student-t distribution (see Eq (6)), where the scaling parameter a and the effective length l are functions of $C(1)$ and L . This approach, however, which is conventional in climate science, can only be considered as a crude approximation since the temperature variability cannot be described by an AR(1) process where the autocorrelation function $C(s)$ decays exponentially with time lag s , but is described by a long-term persistent process where $C(s)$ decays algebraically with s .

In recent years, there have been several attempts to solve the detection problem in long-term persistent data [1, 14, 16, 17, 19–22]. Using Monte Carlo simulations and scaling arguments it was found empirically [1, 22] that for long-term persistent Gaussian data, $P(x; \alpha, L)$ can be approximated reasonably by a Gaussian for small x and by a simple exponential for large x values.

Here we perform the same kind of calculations as in [1, 22], but with a considerably better statistics, and show that the best approximation for P , in the *whole x -regime*, is again the *student-t distribution*, where now the scaling parameter a and the effective length l depend on α and L . While the previous result [1] represents a good approximation in the respective x -windows, the present result is more satisfying since it shows that the distributions of a relative trend in uncorrelated, short-term correlated and long-term correlated data all follow the same equation, namely a student-t-distribution, but with different scaling parameters a and effective lengths l . Accordingly, the exceeding probability W and the significance S of a trend is described, in all these different systems, by the same

hypergeometric function. In addition, we also study P for strongly skewed non-Gaussian data and find that, to a very good approximation, P is the same for all considered distributions. Finally, we apply our methodology to the West-Antarctic temperature record at Byrd station.

The paper is organized as follows: In Section II we describe how the exceedance probability W and the significance S is related to P and which form these quantities have for uncorrelated Gaussian noise and short-term correlated Gaussian data characterized by an AR(1) process. We also give a brief introduction into long-term persistent data and their characterization. In Sections III we present our numerical results for the significance of a relative trend in long-term persistent Gaussian (Section III) and non-Gaussian data (Section IV). In Section V we show how our approach can be applied to monthly temperature records. As an example we take the Byrd record from West Antarctica that has very recently been reconstructed [49]. In Section VI, finally, we summarize our results.

II. DETECTION OF EXTERNAL TRENDS

We consider a record $\{y_i\}, i = 1, \dots, L$ and assume, without loss of generality, that the mean value \bar{y} of the data is zero. To estimate the increase or decrease of the data values in the considered time window of length L , one usually performs a regression analysis. From the regression line $r_i = bi + d$, one obtains the magnitude of the trend $\Delta y = c(L-1)$ as well as the fluctuations around the trend, characterized by the standard deviation $\sigma = [(1/L) \sum_{i=1}^L (y_i - r_i)^2]^{1/2}$. The relevant quantity we are interested in is the *relative trend*

$$x = \Delta y / \sigma. \quad (1)$$

When a certain relative trend has been measured in a data set, the central question is, if this trend may be due to the natural variability of the data set or not ("detection problem"). To solve this problem, one needs to know the probability $P(x; L)dx$ that in model records with the same persistence properties as the considered data set, a relative trend between x and $x + dx$ occurs. The probability density function $P(x; L)$ is symmetric in x . In the following we consider $x > 0$. From P we derive the *exceedance probability* $W(x; L) = \int_x^\infty P(x'; L)dx'$ and the trend significance

$$S(x; L) = \int_{-x}^x P(x'; L)dx' = 1 - 2W(x; L). \quad (2)$$

By definition, S is the probability that the relative trend in the record is between $-x$ and x .

If the significance of a relative trend is above 0.95 (or 95%), one usually assumes that the considered trend cannot be fully explained by the natural variability of the record. The relation $S(x_{95}; L) = 0.95$ defines the upper and lower limits $\pm x_{95}$ of the 95% significance inter-

val (also called confidence interval). By the above assumption, relative trends x between $-x_{95}(L)$ and $x_{95}(L)$ can be regarded as natural. If x is above x_{95} , the part $x - x_{95}$ cannot be explained by the natural variability of the record and thus can be regarded as minimum external relative trend,

$$x_{\text{ext}}^{\min} = x - x_{95}. \quad (3)$$

On the other hand, the external trend cannot exceed

$$x_{\text{ext}}^{\max} = x + x_{95}, \quad (4)$$

which thus represents the maximum external relative trend. By definition, x_{ext}^{\min} represents the lower margin of the observed relative trend that cannot be explained by the natural variability alone, while x_{ext}^{\max} is the largest possible external relative trend consistent with the natural variability of the record. According to Eqs. (3) and (4), $\pm x_{95}(L)$ can be regarded as error bars for an external relative trend in a record of length L .

A. White noise

For uncorrelated Gaussian data (white noise), it has been assumed (see [43] and references therein) that the ratio t_b between the estimated trend slope b and its standard error s_b (see Eqs. (1-5) in [43]) follows a student-t distribution. This assumption can be written as

$$P(x; L) = \frac{\Gamma(\frac{l(L)+1}{2})}{\Gamma(\frac{l(L)}{2})\sqrt{\pi}l(L)a} \left(1 + \frac{(x/a)^2}{l(L)}\right)^{-\frac{l(L)+1}{2}}, \quad (5)$$

with the degrees of freedom

$$l(L) = L - 2 \quad (6)$$

and the scaling parameter

$$a = \frac{\sqrt{12}(L-1)}{\sqrt{L^2+2}} \frac{1}{\sqrt{l(L)}}. \quad (7)$$

Γ denotes the Γ -function. In the limit of large L , a tends to $a \cong \sqrt{12}/\sqrt{l(L)}$.

From (5) and (2) one can obtain straightforwardly the significance trend S as a function of x/a and $l(L)$,

$$S(x; L) = 2 \frac{x}{a} \frac{\Gamma(\frac{1}{2}(l(L)+1))}{\sqrt{\pi}l(L)\Gamma(\frac{l(L)}{2})} \times {}_2F_1\left(\frac{1}{2}, \frac{1}{2}(l(L)+1); \frac{3}{2}; -\frac{(x/a)^2}{l(L)}\right) \quad (8)$$

where ${}_2F_1$ is the hypergeometric function.

B. Short-term correlations

The most basic model for short-term correlations in data sets is the autoregressive process of first order (AR1), where the data satisfy the equation

$$y_{i+1} = c_1 y_i + \eta_i, i = 1, 2, \dots, L - 1. \quad (9)$$

Here, the AR1 parameter c_1 is between -1 and 1 and η_i is white noise. For $c_1 < 0$ the data are antipersistent, while for $c_1 > 0$ they are persistent. For $c_1 = 0$, they are white noise.

For characterizing the persistence of a record, one often studies the autocorrelation function $C(s) = \langle y_i y_{i+s} \rangle \equiv \frac{1}{(L-s)} \sum_{i=1}^{L-s} y_i y_{i+s} / (\frac{1}{L} \sum_{i=1}^L y_i^2)$. By definition, $C(0) = 1$. It is easy to show that for AR1 processes, in the limit of $L \rightarrow \infty$, $C(s)$ decays exponentially, $C(s) = c_1^s$, i.e., c_1 is identical to the lag-1 autocorrelation $C(1)$. For $c_1 > 0$, $C(s)$ can be written as $C(s) = \exp(-s/s_x)$ where $s_x = 1/|\ln c_1|$ denotes the persistence time.

It has been shown [43] that for sufficiently large L where $C(1) = c_1$, P has approximately the form of the student-t distribution Eq. (5), with

$$l(L) = L \frac{1 - C(1)}{1 + C(1)} - 2 \quad (10)$$

and

$$a = \frac{\sqrt{12}(L-1)}{\sqrt{L^2+2}} \frac{1}{\sqrt{l(L)}} \cong \frac{\sqrt{12}}{\sqrt{l(L)}} \quad (11)$$

Accordingly, the significance S of the trend is described by Eq. (8) with $l(L)$ from (10) and a from (11).

C. Long-term persistence

Long-term correlated records can be characterized by the power spectral density $S(f) = |y(f)|^2$, where $\{y(f)\}$, $f = 0, 1, \dots, L/2$, is the Fourier transform of $\{y_i\}$. With increasing frequency f , $S(f)$ decays by a power law,

$$S(f) \sim f^{-\beta}, \quad (12)$$

where $\beta > 0$ characterizes the long-term memory [4]. For white noise, $\beta = 0$. Records with $0 < \beta < 1$ can be characterized by an autocorrelation function $C(s)$ that decays by a power law, $C(s) \sim (1-\gamma)s^{-\gamma}$, with $\gamma = 1-\beta$. To generate long-term persistent data, one usually uses the Fourier-filtering technique based on (12), where long records of uncorrelated Gaussian data (typically of length $L_0 = 2^{21}$) are transformed to Fourier space. The result is multiplied by $f^{-\beta/2}$ and then transformed back to time space. The resulting record is Gaussian distributed. For obtaining records of the desired length L , one divides the long record into segments of length L .

Since both $S(f)$ and $C(s)$ exhibit large finite size effects and are strongly influenced by external deterministic trends, one usually does not use these methods to

characterize the long-term persistence, but prefers methods like the detrending fluctuation analysis of 2nd order (DFA2) [48] where linear trends in the data are eliminated systematically.

In DFA2 one measures the variability of a record by studying the fluctuations in segments of the record as a function of the length s of the segments. Accordingly, one first divides the record $\{y_i\}$, $i = 1, 2, \dots, L$, into non-overlapping windows ν of lengths s . Then one focuses, in each segment ν , on the cumulated sum Y_i of the data and determines the variance $F_\nu^2(s)$ of the Y_i around the best polynomial fit of order 2. After averaging $F_\nu^2(s)$ over all segments ν and taking the square root, we arrive at the desired fluctuation function $F(s)$. One can show that

$$F(s) \sim s^\alpha. \quad (13)$$

The exponent α can be associated with the Hurst exponent, and is related to the correlation exponent γ and the spectral exponent β by $\alpha = (1 + \beta)/2$ and $\alpha = 1 - \gamma/2$. For uncorrelated data, $\alpha = 1/2$. The DFA2 technique gives reliable results for time scales s between 10 and $L/4$ [48].

When applying DFA2 to short-term persistent data, the fluctuation function $F(s)$ approaches a power law, with $\alpha = 1/2$, for s well above the persistence time s_x . For s well below s_x (which can only be the case for b very close to 1), α is close to 1.5. The difference in the functional form of $F(s)$ allows to distinguish between short-term and long-term persistent processes.

Recently, it has been shown [1] by Monte Carlo simulations that in long-term persistent data of length L , where the Hurst exponent α is determined by DFA2, the probability density $P(x; \alpha, L)$ of the relative trend x can be reasonably approximated by a Gaussian for small x and by a simple exponential for large x . Using scaling theory, an analytic expression for $W(x; L)$ has been obtained, as a function of α , in the two x -regimes. Here we follow the same route as in [1], but with a better statistics, and find that the best approximation for P , in the whole x regime, is the student-t-distribution Eq. (5), where the scaling parameter a and the effective length l depend on both α and L .

Accordingly, the significance of a relative trend in long-term persistent records is described by the same hypergeometric function as for white noise and AR1 noise, only the parameters l and a are different. We also show that the results derived for Gaussian data hold, in an excellent approximation, also for data with a symmetric exponential distribution $D(y) = (1/2)\exp(-|y|)$ as well as for strongly skewed distributions like the one-sided exponential and one-sided power-law distribution.

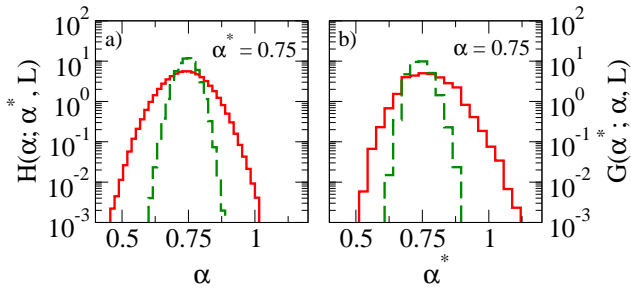


FIG. 1. (color online) (a) When long data sets with global Hurst exponents α^* (created by Fourier filtering) are divided into sub-segments of length L , the local Hurst exponents α vary around α^* . The figure shows the distribution $H(\alpha; \alpha^*, L)$ of the local Hurst exponents α (obtained by DFA2) in segments of length $L = 400$ (continuous red line) and $L = 2200$ (dashed green line), for fixed global Hurst exponent $\alpha^* = 0.75$. (b) According to (a), the same local Hurst exponent α can originate from long data sets with different global Hurst exponents α^* . The figure shows, for the local Hurst exponent $\alpha = 0.75$ in segments of length $L = 400$ (continuous red line) and $L = 2200$ (dashed green line), the distribution $G(\alpha^*; \alpha, L)$ of the involved global Hurst exponents α^* .

III. SIGNIFICANCE OF TRENDS IN LONG-TERM CORRELATED GAUSSIAN DATA SETS

For determining $P(x; \alpha, L)$ numerically, we follow [1]. We use the Fourier-filtering technique [2] to generate 800 synthetic records of length 2^{21} , for 241 global Hurst exponents α^* ranging from $\alpha^* = 0.1$ to $\alpha^* = 2.5$. We are interested in data sets with lengths L between 400 and 2200 which correspond, in monthly temperature data sets, to data lengths between 33 and 183 years. Accordingly, we divided each data set into subsequences of lengths $L = 400, 500, 600, \dots, 2200$. In each subrecord of length L , we used linear regression to determine (i) the local DFA2 Hurst exponent α as the slope of the regression line in a double logarithmic presentation of the fluctuation function $F(s)$ between $s = 10$ and $L/4$ and (ii) the relative trend x . We are interested in α values between 0.5 and 1.5, which are most common in nature.

It has been noticed before [1, 18, 22], that the local Hurst exponents α obtained in each subrecord are not identical to the global Hurst exponent α^* of the entire record, but vary around α^* . The distribution of the local Hurst exponents α , for fixed $\alpha^* = 0.75$ and $L = 400$ and 2200, is shown in Fig. 1a. As expected, the distribution narrows with increasing subrecord length L . Accordingly, when in a subrecord a certain local Hurst exponent α is measured, the subrecord may be part of a long data set with a different global Hurst exponent α^* . Figure 1b shows, for fixed $\alpha = 0.75$, the distribution of the α^* values. Again, the distribution narrows with increasing L . As a consequence, for determining the significance of

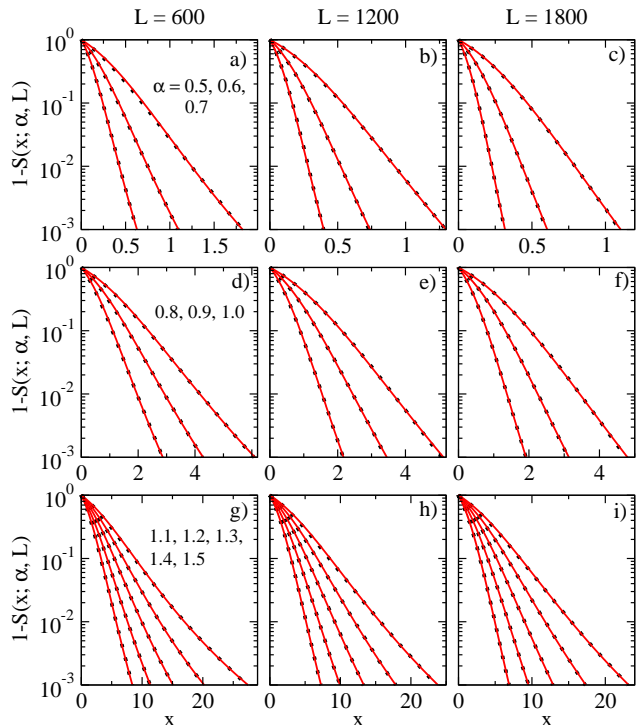


FIG. 2. (color online) Significance $S(x; \alpha, L)$ of relative trends x occurring in long term correlated data of length L and Hurst exponent α . The data are Gaussian distributed. For clarity, we focus on $1 - S$. (a) is for $L = 600$ and $\alpha = 0.5, 0.6, 0.7$ (symbols from bottom to top). The continuous lines show the corresponding student-t-fits. (b,c) Same as (a) but for the Hurst exponents $\alpha = 0.8, 0.9, 1.0$ and $\alpha = 1.1, 1.2, 1.3, 1.4, 1.5$, respectively. (d-f) and (g-i): Same as (a-c) but for record lengths $L = 1200$ and $L = 1800$, respectively.

a relative trend in a long-term correlated record of length L , one cannot simply identify the local Hurst exponents α with the global one, but has to determine the local Hurst exponents in each subrecord separately. As we will show in the second part of this Section, ignoring this fact will lead to a strongly enhanced significance. We like to note that a similar problem occurs in short-term persistent records, where only in long data sets the lag-1 autocorrelation function $C(1)$ is equal to the persistence parameter b . In subrecords (or short data sets) of length L , the values of $C(1)$ fluctuate around b , and Eqs. (10) and (11) are not valid [28].

After having obtained in each subrecord k (of fixed length L) the local Hurst exponents α_k , we focus on those subrecords that have local α values between 0.49 and 1.51. We divide the local α values into 51 windows of length 0.02, such that in the first window $\alpha = 0.5 \pm 0.01$, in the second window $\alpha = 0.52 \pm 0.01$, and in the last window $\alpha = 1.5 \pm 0.01$. Then we determine, in each α -window, the distribution $P(x; \alpha, L)$ of the relative trends as well as the trend significance S .

Figure 2 shows $1 - S(x; \alpha, L) = 2W(x; \alpha, L)$ for three

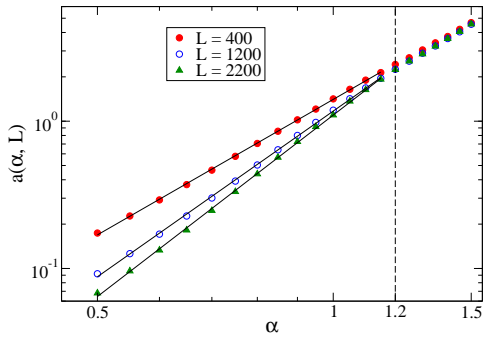


FIG. 3. (color online) The characteristic relative trend $a(\alpha, L)$ that characterizes the decay of $1 - S$ (see Fig. 2 and Eq. (??)), as a function of the Hurst exponent α for three record lengths $L = 400, 1200, 2200$. The straight lines are power law fits between $\alpha = 0.5$ and 1.15 .

representative data lengths $L = 600, 1200$, and 1800 , which in monthly climate records correspond to 50, 100, and 150 years. The dots are our numerical results. The continuous lines result from a fit of S to Eq. (8), with appropriately chosen values for the scaling parameter a and the effective length l . The figure shows that over all three decades of $1 - S$ considered here (where S ranges from 0 to 0.999 (or from 0 to 99.9 %)), the fit is excellent. The parameters l and a are listed, for L between 400 and 2200, in the Appendix.

Table 1 in the Appendix shows that for fixed record length L , the effective length l is a constant in the most relevant range between $\alpha = 0.5$ and 1.1 . For example, for $L = 600, 1200$, and 1800 , $l = 9.24, 12.05$, and 13.69 , respectively. For α above 1.1 , $l(L)$ decreases strongly.

Figure 3 shows that the scaling parameter a listed in Table 2 in the Appendix, can be approximated, for α between 0.5 and 1.2 , by a power law, where the slope increases with increasing L . Above $\alpha = 1.2$, a shows only a very weak L dependence.

From Fig. 2, by intersecting $1 - S$ with the constant 5×10^{-2} , we obtain immediately the relative trend x_{95} that is conventionally used to estimate the error bars of a measured relative trend. Figure 4 shows x_{95} for $L = 600, 1200$ and 1800 . From the figure, one can immediately read off the error bars of a relative temperature trend in monthly records of length 50, 100, and 150 years with DFA2 exponent α , and specify its lower and upper bounds $x_{\text{ext}}^{\min} = x - x_{95}$ and $x_{\text{ext}}^{\max} = x + x_{95}$.

Finally, at the end of this Section, let us go back to its beginning and ask the following question: Given a long record of length L_0 described by the global Hurst exponent α^* , which is divided into subrecords of length $L \ll L_0$. What is the significance $\tilde{S}(x; \alpha^*, L)$ of a relative trend x in these subrecords? We expect that for large L where all local Hurst exponents α are very close to α^* , $\tilde{S}(x, \alpha^*, L)$ and $S(x, \alpha, L)$ will coincide. For small L we expect that $\tilde{S}(x, \alpha^*, L)$ overestimates the significance.

The difference between $S(x, \alpha, L)$ and $\tilde{S}(x, \alpha^*, L)$ may

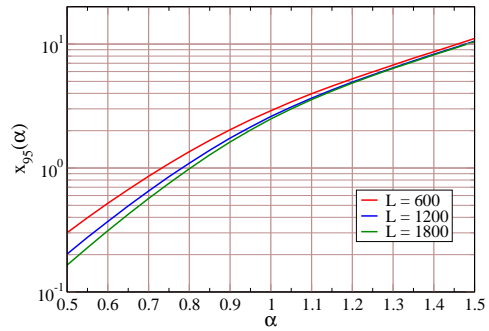


FIG. 4. (color online) The relative trend x_{95} corresponding to the 95% significance level as a function of the Hurst exponent α for the segment lengths $L = 600, 1200$, and 1800 (from top to bottom). By definition, x_{95} is obtained from the intersection of $1 - S$ in Fig. 2 with $1 - 0.95 = 0.05$.

also be regarded as follows: If we know a priori that the considered data set is characterized by a certain Hurst exponent (which is the case, for example, when we consider records consisting of Gaussian distributed independent random numbers or their cumulated sum), then $\tilde{S}(x, \alpha^*, L)$ gives the proper significance. If we do not know the characteristics of the data set a priori, the uncertainty is increased and we have to determine explicitly its Hurst exponent, $S(x, \alpha, L)$ gives the proper significance.

Figure 5 shows $\tilde{S}(x, \alpha^*, L)$ for the global Hurst exponents $\alpha^* = 0.5, 0.75, 1$, and 1.25 in subrecords of lengths $L = 400, 1200$, and 2200 . The figure shows also the significance $S(x, \alpha, L)$, for $\alpha = 0.5, 0.75, 1$, and 1.25 . For $\alpha^* = 0.5$, $\tilde{S}(x, \alpha^*, L)$ follows Eq. (8) with (6) and (7). We found that also for $\alpha = 0.75$ and 1 , $\tilde{S}(x, \alpha^*, L)$ is well described by the student-t distribution (8) with $l(L) = L - 2$ (6). For $\alpha = 0.75$, the a values are $0.512, 0.383$, and 0.328 for $L = 400, 1200$ and 2200 , respectively. For $\alpha = 1$, the respective a values are $1.313, 1.185$, and 1.135 . As expected, $\tilde{S}(x, \alpha^*, L)$ overestimates the significance of an observed relative trend and thus underestimates the error bars $\pm x_{95}$ of a relative trend. For example, when in a monthly temperature record of length 600 (corresponding to 50 years) characterized by $\alpha = 0.75$ a relative trend $x = 1$ is measured, the proper significance of this trend is $S = 0.94$, i.e. the trend is not significant. However, if falsely \tilde{S} is used for estimating the significance, one overestimates the significance, since $\tilde{S} = 0.975$ in this case.

IV. SIGNIFICANCE OF TRENDS IN LONG-TERM CORRELATED NON-GAUSSIAN DATA SETS

By using the Fourier-filtering technique we generated long-term correlated Gaussian data $\{y_i\}$. Many natural records, e.g., monthly temperature anomalies where

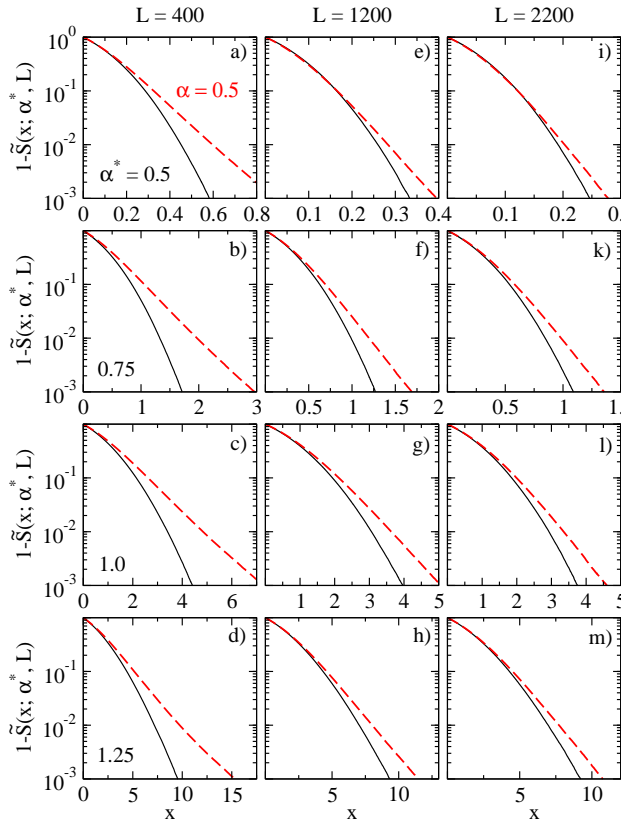


FIG. 5. (color online) Significance $\tilde{S}(x; \alpha^*, L)$ of relative trends x occurring in segments of length N of long data s (length 2^{21}) with fixed global Hurst exponent α^* (conting line). The data follow Gaussian distributions. For clarity, we focus on $1 - S$, as in Fig. 2. We compare $\tilde{S}(x; \alpha^*, L)$ with the significance $S(x; \alpha, L)$ of relative trends x occurring in data sets of the same length N with fixed local Hurst exponent α (dashed red line) that was shown in Fig. 2. The considered segment lengths are $L = 400, 1200$, and 2200 , shown columns 1 – 3. The Hurst exponents $\alpha^* = \alpha$ are $0.5, 0.75, 1.0$, and 1.25 , shown in rows 1 – 4.

the seasonal trend has been removed, are Gaussian distributed. But others, like river run-off data, have a quite skewed distribution and cannot be characterized by a Gaussian [35, 36]. Accordingly, the question arises, to which extent our results derived in the previous subsection are general and apply also to non-Gaussian distributions.

To answer this question, we have considered three kinds of non-Gaussian distributions: (i) the symmetric exponential distribution $D(y) = (1/2) \exp(-|y|)$, (ii) the (highly skewed) exponential distribution $D(y) = \exp(-y), y \geq 0$, and (iii) the (highly skewed) power law distribution $D(y) = y^{-5}, y \geq 0$. To generate these distributions, we have first generated long-term correlated data $\{y_i\}$ of length 2^{21} that are Gaussian distributed, as above. Then we generated 2^{21} data of the considered non-Gaussian distribution and exchanged the long-term

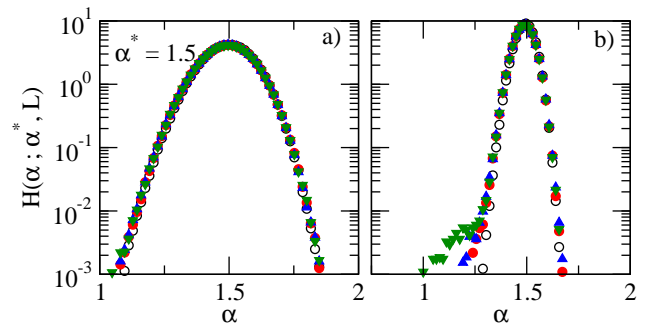


FIG. 6. (color online) Distribution $H(\alpha; \alpha^*, L)$ of local Hurst exponents α (obtained by DFA2) in segments of length $L = 400$ and $L = 2200$, for fixed global Hurst exponents $\alpha^* = 1.5$. $H(\alpha; \alpha^*, L)$ has been obtained for data following a Gaussian distribution (open circles), an exponential distribution (full circles), a symmetric exponential distribution (triangle up), and a power law distribution (triangle down). The non-Gaussian data have been generated by the exchange technique.

correlated Gaussian data rankwise by the non-Gaussian data.

By this simple exchange technique we obtain long-term correlated data following the considered non-Gaussian distribution, but the global Hurst exponent as well as the local ones usually differ slightly from the original one. These slight deviations do not play a role here, since we consider α^* values between 0.1 and 1.9 and only the *local* α values measured by DFA2 are essential in our analysis. If one needs to obtain data with exactly the same α^* value as the Gaussian data, one has to use the iterative Schreiber-Schmitz procedure [51], where in each iteration the data are (1) Fourier-transformed to f space. Then (2) the Fourier-transformed data are exchanged by the Fourier-transform of the original Gaussian data and (3) Fourier-transformed back to time space. Finally, (4) these data are exchanged rankwise by the desired non-Gaussian distribution. By comparing the simple exchange method with the Schreiber-Schmitz procedure we found that both methods yield, for the same global Hurst exponent $\alpha^* \leq 1.5$, the same distribution $H(\alpha; \alpha^*, L)$ of local Hurst exponents α as the Gaussian records.

Figure 6 shows, for $\alpha^* = 1.5$ and $L = 400$ and 2200 , the distributions $H(\alpha; \alpha^*, L)$ of local Hurst exponents α for both Gaussian and non-Gaussian data. Above $\alpha^* = 1.5$, we were unable to generate long-term correlated records with the considered non-Gaussian distributions. Irrespective of the input value of α^* , the output α^* was always close to 1.5 , and the distribution of the α values became much broader than for the Gaussian data. Accordingly, our analysis of non-Gaussian data is limited to those α values that are typically absent in long records with $\alpha_c(L) = 1.15, 1.31$, and 1.34 , respectively, where the fraction of subrecords originating from long records with

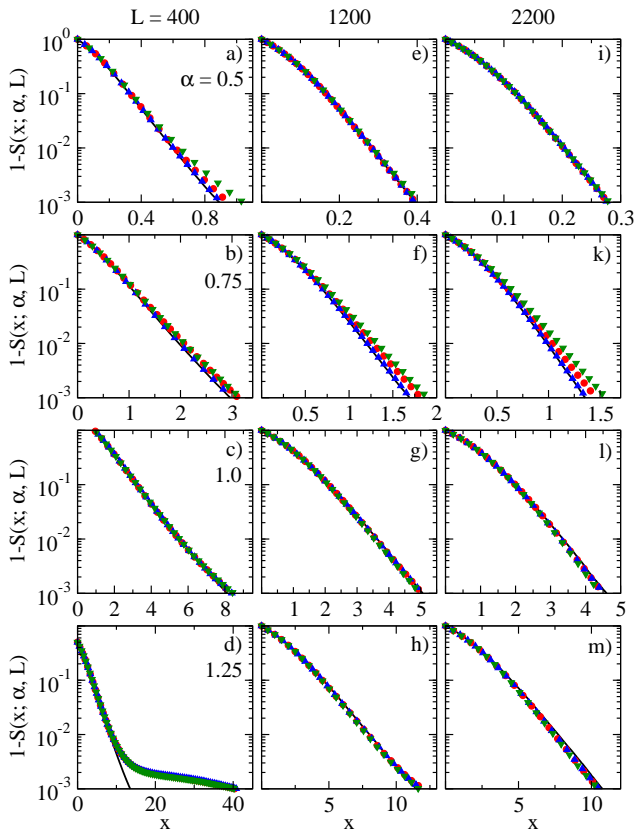


FIG. 7. (color online) Dependence of the significance $S(x, \alpha, L)$ of the relative trend x on the distribution of the long-term persistent data. Apart from Gaussian data (continuous line, shown also in Fig. 2), we consider data with asymmetric exponential distribution (full circle), symmetric exponential distribution (triangle up), and power law distribution (triangle down). For convenience, we show $1 - S$ as in Fig. 2. The record lengths are $L = 400, 1200,$ and 2200 (columns 1 – 3), and the Hurst exponents are $\alpha = 0.5, 0.75, 1,$ and 1.25 (rows 1 – 4).

α^* above 1.5, is below 10^{-3} . Accordingly, our analysis holds only for local Hurst exponents α below $\alpha_c(L)$.

Figure 7 shows the significance of the relative trend x for the 3 non-Gaussian distributions considered here, for $L = 400, 1200,$ and 2200 . The continuous line (difficult to see) is the result for the Gaussian data. The figure shows that for α below 1 (rows 1 – 3 in the figure), the data for the two-sided exponential distribution fully coincide with the Gaussian data, while there are minor deviations for the strongly skewed data. It is important to note that $1 - S$ of the Gaussian distribution appears to be a lower bound for $1 - S$ of the skewed distributions, this means that the significance of a trend in long-term correlated Gaussian data represents an upper bound for the significance.

Accordingly, the value obtained for x_{95} in Gaussian distributed data represents a lower bound, but the differences between the different distributions are very small,

the largest deviations occur for $\alpha = 0.75$ and $L = 2200$ where x_{95} for the skewed power-law distribution exceeds x_{95} for the Gaussian distribution by less than 5 percent. For $\alpha = 1$, x_{95} is the same for all distributions. For $\alpha = 1.25$ (last row) which is below α_c for $L = 1200$ and 2200 , the agreement between Gaussian and non-Gaussian data is perfect for $L = 1200$ and 2200 . For $L = 400$, where α is above α_c and thus should not be considered, Gaussian and non-Gaussian data still collapse for $1 - S$ above 10^{-2} . The shoulder below 10^{-2} is an artifact which originates from records where the original α^* value was above 1.5.

V. EXAMPLE: THE ANTARCTIC BYRD RECORD

It is straightforward to apply our methodology to observational data. Important applications are climate data (e.g., river flows, precipitation, and temperature data) where one likes to know the significance of trends due to anthropogenic climate change. When considering climate data, it is important to use monthly data where additional short-term dependencies have been averaged out and seasonal trends can be better eliminated than in daily data [1].

For convenience we consider temperature data. The seasonal trend elimination is done in 2 steps [35, 36]. In the first step, we subtract the monthly seasonal trend to obtain the temperature anomalies $\tilde{y}_i, i = 1, \dots, L$. Since the variance of the temperature anomalies may depend on the season, we divide in the second step the temperature anomalies by the seasonal standard deviation. The resulting dimensionless record y_i has unit variance and zero mean.

Next we perform the regression analysis for the $\{y_i\}$ which yields Δ and σ and thus the relative trend x . Then we employ DFA2 and obtain the Hurst exponent α . From x and α we can estimate the significance S of the temperature trend from Tables I and II as well as the boundary $\pm x_{95}$ of the 95% significance interval.

Since we divided the temperature anomalies by the seasonal standard deviation to obtain $\{y_i\}$, Δ and σ as well as the error bars $\pm \Delta_{95} = x_{95} \sigma$ are dimensionless. To obtain the real trend Δ^{real} and its real error bars $\pm \Delta_{95}^{\text{real}}$ in units of $^{\circ}\text{C}$, we perform a regression analysis of the temperature anomalies $\tilde{y}_i, i = 1, \dots, L$. To obtain the error bars $\Delta_{95}^{\text{real}}$ we use the identity (see [1]) $\Delta_{95}^{\text{real}} / \Delta^{\text{real}} = \Delta_{95} / \Delta$, which then yields

$$\Delta_{95}^{\text{real}} = \Delta_{95} \frac{\Delta^{\text{real}}}{\Delta}.$$

The resulting minimum and maximum external temperature trends are $\Delta^{\text{real}} \pm \Delta_{95}^{\text{real}}$.

To show explicitly how our approach can be used to estimate the significance of a warming trend we consider the monthly (corrected) Byrd record between 1957 and 2013 that was recently reconstructed by Bromwich et

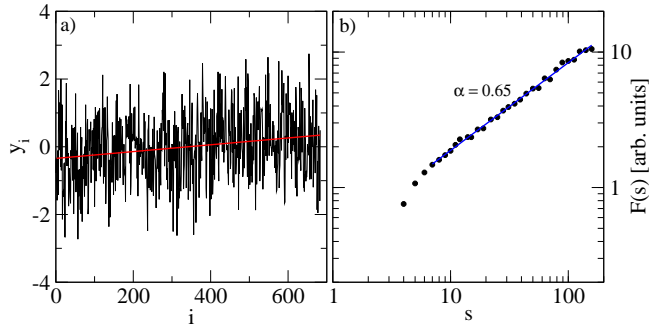


FIG. 8. (color online) (a) Monthly fully seasonally detrended record y_i at the Byrd station between 1957 and 2013 (black lines) and the corresponding linear regression (red line). (b) The DFA2 fluctuation function $F(s)$ of the monthly Byrd record y_i (black circles).

al. [50]. (An earlier version [46] of the Byrd record has been discussed in [28]). The Byrd station is located in the center of West Antarctica which is one of the fastest warming places on Earth. The regression analysis yields $\Delta^{\text{real}} = 2.02^\circ\text{C}$. It is obvious that the question of the significance of Antarctic warming is highly relevant, since the warming trend influences the melting of the West Antarctic Ice Shield and thus contributes to future sea level rise.

Figure 8a shows the fully seasonally detrended Byrd record y_i , $i = 1, \dots, 684$, where the temperature anomalies have been divided by the seasonal standard deviation. The regression analysis yields $\Delta = 0.69$ and $\sigma = 1.04$, yielding $x = 0.66$.

Figure 8b shows the result of the DFA2 analysis for y_i (full circles). In the double logarithmic plot, the DFA2 fluctuation function $F(s)$ follows a straight line with exponent $\alpha = 0.65$ between $s = 10$ and $L/4$. Accordingly, the data are long-term persistent and our methodology applies. The exponent $\alpha = 0.65$ is in agreement with earlier estimates [28, 50]. We like to note that the temperature anomalies \tilde{y}_i yield to the same Hurst exponent showing explicitly that the second step in the seasonal detrending has no influence on the persistence properties.

For obtaining the degrees of freedom l and the scaling factor a for $\alpha = 0.65$ and $L = 684$, we consider the 4th line in Table 1 and 2 and use the respective values for $L = 500, 600, 700$ and 800 for a cubic interpolation. This gives $l = 9.78$ and $a = 0.286$. Inserting these values into Eq. (9) gives $S = 0.953$ and $x_{95} = 0.64$. Accordingly, the significance of the warming trend at the Byrd station is 95.3%. The minimum external trend is 0.03°C , while the maximum external trend is 3.99°C .

When Bromwich et al determined these quantities, they used the conventional hypothesis that the *annual* linearly detrended temperature data follow an AR(1) process and that S can be obtained from Eqs. (9), (11) and (12) (even though the length of the annual data is

too small to make (11) and (12) applicable). For the annual detrended data, they obtained $C(1) = 0.075$ and thus $l = 49.05$ and $a = 0.546$. Inserting the corresponding values into (9) yields $S = 0.999$ and $x_{95} = 0.997$. The minimum external trend is 0.87°C , while the maximum external trend is 3.09°C .

Accordingly, the significance of the warming trend as well as the minimum external trend has been strongly overestimated by Bromwich et al, while the uncertainty $2x_{95}$ has been underestimated.

VI. CONCLUSIONS

In summary, we have studied by extensive Monte-Carlo simulations the distribution $P(x; \alpha, L)$ of linear trends in long-term correlated records of length L that are characterized by a Hurst exponent α between 0.5 and 1.5 (determined by DFA2). The Hurst exponent was obtained by linear regression from the slope of the regression line in a double logarithmic representation of the DFA2 fluctuation function $F(s)$ between $s = 10$ and $L/4$. We have considered record lengths L between 400 and 2200, which corresponds, in monthly climate records, to time scales between 33.3 and 183.3 years. In each record we have determined by linear regression analysis the increase Δ and the standard deviation σ of the data around the regression line; the ratio $x = \Delta/\sigma$ is the relative trend.

We have extended the earlier analysis [1] in three important directions:

(i) We found that $P(x; \alpha, L)$ follows, in the whole x -range, the student-t distribution with two fit parameters, the scaling parameter a and the effective length l . This generalizes nicely the known results for white noise and AR(1) processes, where P also follows a student-t distribution, but with different a and l values. For Hurst exponents between 0.5 and 1.1, l depends only on the record length L , and not on the Hurst exponent α . In the previous work [1], the distribution was approximated by a Gaussian at small x and an exponential at large x values, which allowed to determine easily the significance of large relative trends.

(ii) In [1], only Hurst exponents up to 1.1 could be treated analytically. Here we extend the analytical analysis to $\alpha = 1.5$ where the deviations from simple exponential behavior at large x are more pronounced. We also considered slightly smaller and larger record lengths.

(iii) In [1], only Gaussian data were considered. Here we have shown explicitly that the results are stable and do hold also for very different, highly skewed distributions.

For applying our methodology to observable data one must be sure that there are no additional short term correlations on short time scales. It is known that in temperature anomalies, there are additional short term correlation on time scales up to 10 days. For river flows, the short term persistence may range up to one month. These short term correlations can be eliminated by aver-

aging the data over short time windows that are larger than the persistence time, i.e. by considering monthly temperature anomalies and quarter annual river flows. The DFA2 analysis then has to be performed on these averaged records and the actual data length L is the length of the averaged data set.

In long-term persistent processes it is enough to determine α by DFA2 and use this value to determine a and l . In most previous evaluations of the significance of trends in climate science the significance of trends has been determined from the value of $C(1)$ in annual records, assuming that the significance of trends in an AR(1) record may be a good approximation for the significance of trends in long-term correlated climate records. Our results show that one does not need to rely on this crude approximation (which usually strongly exaggerates the significance) since the estimation of the significance of trends in long-term correlated records is not more difficult.

Acknowledgements: We like to thank the Deutsche Forschungsgemeinschaft and the Ministry of Education and Science of the Russian Federation for financial support.

VII. APPENDIX

We have shown in this article that the probability $P(x; \alpha, L)$ that in a long-term persistent record of length L , characterized by the Hurst exponent α , a relative trend of strength x occurs, has the form of a student-t distribution,

$$P(x; \alpha, L) = \frac{\Gamma(\frac{l+1}{2})}{\Gamma(\frac{l}{2})\sqrt{\pi l a}} \left(1 + \frac{(x/a)^2}{l}\right)^{-\frac{l+1}{2}},$$

with the effective length l and the scaling parameter a . The related trend significance is

$$S(x; \alpha, L) = 2 \frac{x}{a} \frac{\Gamma(\frac{1}{2}(l+1))}{\sqrt{\pi l} \Gamma(\frac{l}{2})} {}_2F_1\left(\frac{1}{2}, \frac{1}{2}(l+1); \frac{3}{2}; -\frac{(x/a)^2}{l}\right).$$

Tables I and II list the effective lengths l and the scaling factor a as function of the DFA2 Hurst exponent α and the record length l .

-
- [1] S. Lennartz and A. Bunde, Phys. Rev. E., **84**, 021129 (2011).
- [2] B. B. Mandelbrot, *Gaussian Self-Affinity and Fractals* (Springer, New York, Berlin, Heidelberg, 2001)
- [3] P. Bloomfield, and D. Nychka, Climatic Change, **21**, 275 (1992).
- [4] J. D. Pelletier and D. L. Turcotte, J. Hydrology, **203**, 198 (1997).
- [5] E. Koscielny-Bunde et al., Phys. Rev. Lett., **81**, 729 (1998).
- [6] B. D. Malamud and D. L. Turcotte, Advances in Geophysics, **40**, 1 (1999).
- [7] P. Talkner and R.O. Weber, Phys. Rev. E, **62**, 150, DOI:10.1103/PhysRevE.62.150 (2000).
- [8] R.O. Weber and P. Talkner, J. Geophys. Res. **106**, 20131 (2001).
- [9] R.A. Monetti, S. Havlin, and A. Bunde, Physica A **320**, 581 (2003).
- [10] J. Eichner, E. Koscielny-Bunde, A. Bunde, S. Havlin, and H. J. Schellnhuber, Phys. Rev. E, **68**, 046133 (2003).
- [11] K. Fraedrich and R. Blender, Phys. Rev. Lett. **90**, 108501 (2003).
- [12] R. Blender and K. Fraedrich, Geophys. Res. Lett., **30**, 1769 (2003).
- [13] L. A. Gil-Alana, J. Climate, **18**, 5357 (2005).
- [14] T.A. Cohn and H.F. Lins, Geophys. Res. Lett., **32**, L23402 (2005).
- [15] A. Király, I. Bartos, and I.M. Jánosi, Tellus, **58A**, 5, 593, (2006).
- [16] D. Rybski, A. Bunde, S. Havlin and H. von Storch, Geophys. Res. Lett. **33**, L06718 (2006).
- [17] E. Giese, I. Mossig, D. Rybski, and A. Bunde, Erdkunde **61**, 186 (2007).
- [18] D. A. Rybski, A. Bunde, and H. v. Storch, J. Geophys. Res. Atmospheres, **113**, D02106 (2008).
- [19] E. Zorita, T.F. Stocker, and H. v. Storch, Geophys. Res. Lett. **35**, L24706 (2008).
- [20] D. Rybski and A. Bunde, Physica A **388**, 1687 (2009).
- [21] J.M. Halley, Physica A **388**, 2492 (2009).
- [22] S. Lennartz, and A. Bunde, Geophys. Res. Lett., **36**, L16706 (2009).
- [23] S. Fatichi, S. M. Barbosa, E. Caporali, and M. E. Silva, J. Geophys. Res., **114**, D18121 (2009).
- [24] C. Franzke, J. Climate, **23**, 6074 (2010).
- [25] C. Franzke, C., J. Climate, **25**, 4172 (2012).
- [26] S. Lovejoy and D. Schertzer, in: Extreme events and natural hazards: the complexity perspective, A.S. Sharma, A. Bunde, D. Baker, and V.P. Dimri (eds), AGU monographs, 231 (2012).
- [27] C. Franzke, Geophys. Res. Lett., **40**, 1391 (2013).
- [28] A. Bunde, J. Ludescher, C. Franzke, and U. Büntgen, Nature Geoscience, **7**, 246 (2014).
- [29] H. E. Hurst, Transactions of the American Society of civil engineers, **116**, 770 (1951).
- [30] B. B. Mandelbrot and J. R. Wallis, Water Resources Research, **4**, 5, 909 (1968).
- [31] A. Montanari, R. Rosso, and M. S. Taqqu, Water Resources Research, **36**, 5, 1249 (2000).
- [32] A. Montanari, Theory and Application of Long-range Dependence, P. Doukhan, G. Oppenheim, M. S. Taqqu, Eds., 461-472 (2003).
- [33] D. Koutsoyiannis, Hydrological Sciences J. **48**, 3 (2003).
- [34] D. Koutsoyiannis, J. Hydrology **322**, 25 (2006).

$\alpha \backslash L$	L400	L500	L600	L700	L800	L900	L1000	L1200	L1400	L1600	L1800	L2000	L2200
0.50	7.60	8.50	9.24	9.87	10.41	10.88	11.31	12.05	12.67	13.21	13.69	14.11	14.50
0.55	7.60	8.50	9.24	9.87	10.41	10.88	11.31	12.05	12.67	13.21	13.69	14.11	14.50
0.60	7.60	8.50	9.24	9.87	10.41	10.88	11.31	12.05	12.67	13.21	13.69	14.11	14.50
0.65	7.60	8.50	9.24	9.87	10.41	10.88	11.31	12.05	12.67	13.21	13.69	14.11	14.50
0.70	7.60	8.50	9.24	9.87	10.41	10.88	11.31	12.05	12.67	13.21	13.69	14.11	14.50
0.75	7.60	8.50	9.24	9.87	10.41	10.88	11.31	12.05	12.67	13.21	13.69	14.11	14.50
0.80	7.60	8.50	9.24	9.87	10.41	10.88	11.31	12.05	12.67	13.21	13.69	14.11	14.50
0.85	7.60	8.50	9.24	9.87	10.41	10.88	11.31	12.05	12.67	13.21	13.69	14.11	14.50
0.90	7.60	8.50	9.24	9.87	10.41	10.88	11.31	12.05	12.67	13.21	13.69	14.11	14.50
0.95	7.60	8.50	9.24	9.87	10.41	10.88	11.31	12.05	12.67	13.21	13.69	14.11	14.50
1.00	7.60	8.50	9.24	9.87	10.41	10.88	11.31	12.05	12.67	13.21	13.69	14.11	14.50
1.05	7.60	8.50	9.24	9.87	10.41	10.88	11.31	12.05	12.67	13.21	13.69	14.11	14.50
1.10	7.60	8.50	9.24	9.87	10.41	10.88	11.31	12.05	12.67	13.21	13.69	14.11	14.50
1.15	7.06	7.69	8.86	9.32	9.63	10.51	11.08	11.76	13.12	12.50	13.07	14.24	14.44
1.20	6.95	7.50	8.27	9.54	9.21	9.63	10.28	11.14	11.91	11.92	12.48	13.13	14.26
1.25	6.41	7.32	7.91	8.74	8.61	9.27	9.85	10.55	11.21	11.34	11.59	12.44	12.94
1.30	6.25	6.68	7.60	8.11	8.28	8.55	9.28	9.90	10.21	10.36	10.74	11.26	11.03
1.35	5.93	6.31	7.29	7.68	7.83	8.21	8.74	9.12	9.88	9.88	10.26	10.40	10.40
1.40	5.47	5.80	6.63	7.21	7.44	7.55	7.93	8.49	8.94	8.78	9.02	9.48	9.74
1.45	5.19	5.54	6.33	6.83	6.83	7.14	7.58	7.82	8.62	8.18	8.43	8.80	9.01
1.50	4.77	5.10	5.88	6.45	6.33	6.76	6.88	7.42	7.48	7.55	7.76	8.25	8.41

TABLE I. Effective length $l(\alpha, L)$ in the trend distribution P and the trend significance S in long term correlated data with Hurst exponent α and record length L .

$\alpha \backslash L$	L400	L500	L600	L700	L800	L900	L1000	L1200	L1400	L1600	L1800	L2000	L2200
0.50	0.174	0.162	0.133	0.124	0.115	0.107	0.104	0.092	0.086	0.081	0.076	0.072	0.068
0.55	0.227	0.212	0.177	0.165	0.154	0.145	0.140	0.126	0.117	0.111	0.105	0.100	0.096
0.60	0.292	0.275	0.232	0.218	0.205	0.193	0.188	0.171	0.160	0.153	0.145	0.139	0.133
0.65	0.371	0.352	0.300	0.284	0.268	0.256	0.249	0.227	0.215	0.206	0.196	0.190	0.182
0.70	0.465	0.447	0.385	0.368	0.348	0.332	0.325	0.301	0.286	0.275	0.265	0.256	0.247
0.75	0.577	0.556	0.486	0.466	0.446	0.428	0.420	0.392	0.376	0.364	0.351	0.341	0.332
0.80	0.706	0.687	0.606	0.585	0.564	0.543	0.537	0.504	0.486	0.473	0.460	0.448	0.438
0.85	0.854	0.835	0.745	0.726	0.703	0.681	0.675	0.639	0.621	0.609	0.593	0.582	0.568
0.90	1.021	1.006	0.906	0.883	0.864	0.841	0.833	0.800	0.778	0.769	0.752	0.742	0.726
0.95	1.208	1.198	1.088	1.069	1.051	1.026	1.021	0.981	0.961	0.952	0.937	0.924	0.917
1.00	1.417	1.410	1.291	1.276	1.256	1.233	1.229	1.187	1.171	1.167	1.151	1.142	1.100
1.05	1.646	1.648	1.517	1.506	1.488	1.466	1.456	1.420	1.409	1.404	1.390	1.340	1.366
1.10	1.900	1.915	1.776	1.758	1.745	1.722	1.716	1.681	1.666	1.670	1.657	1.590	1.633
1.15	2.138	2.133	2.024	2.016	1.992	1.985	1.993	1.953	1.971	1.938	1.937	1.938	1.925
1.20	2.427	2.420	2.288	2.327	2.273	2.261	2.268	2.248	2.244	2.238	2.237	2.231	2.238
1.25	2.695	2.758	2.584	2.615	2.568	2.569	2.580	2.556	2.559	2.561	2.548	2.552	2.557
1.30	3.045	3.044	2.917	2.927	2.906	2.884	2.915	2.893	2.883	2.887	2.886	2.887	2.857
1.35	3.404	3.411	3.286	3.287	3.264	3.252	3.279	3.242	3.267	3.261	3.263	3.239	3.228
1.40	3.758	3.750	3.621	3.662	3.665	3.619	3.637	3.640	3.643	3.626	3.630	3.624	3.635
1.45	4.202	4.234	4.052	4.102	4.062	4.060	4.101	4.042	4.097	4.061	4.055	4.065	4.060
1.50	4.666	4.679	4.538	4.615	4.534	4.554	4.546	4.550	4.514	4.535	4.530	4.560	4.561

TABLE II. Scaling factor $a(\alpha, L)$ in the trend distribution P and the trend significance S in long term correlated data with Hurst exponent α and record length L .

- [35] J. W. Kantelhardt, E. Koscielny-Bunde, D. Rybski, P. Braun, A. Bunde, and S. Havlin, *J. Geophys. Res. Atmospheres*, **111**, D01106 (2006).
- [36] E. Koscielny-Bunde, J. W. Kantelhardt, P. Braun, A. Bunde, and S. Havlin, *J. of Hydrology.*, **322**, 120 (2006).
- [37] A. Beretta, H. E. Roman, F. Ricich, and F. Crisciani, *Physica A*, **347**, 695 (2005).
- [38] S. Dangendorf et al. *Geophys. Res. Lett.* **41**, 15, 5530 (2014).
- [39] M. Becker, M. Karpytchev, and S. Lennartz-Sassinek, *Geophys. Res. Lett.* **41**, 15, 5571 (2014).

- [40] K. Hasselmann, *J. Climate* **6**, 1957 (1993).
- [41] G.C. Hegerl, H. von Storch, K. Hasselmann, B.D. Santer, U. Cubasch, and P.D. Jones *J. Climate* **9**, 2281 (1996).
- [42] F. W. Zwiers, in *Antropogenic Climate Change* (Springer, New York, 1999), pp. 163-209
- [43] B. D. Santer et al., *J. Geophys. Res. Atmospheres*, **105**, 7337 (2000).
- [44] J. Turner, *Int. J. Climatol.*, **25**, 279 (2005).
- [45] E. J. Steig, *Nature*, **457**, 459 (2009).
- [46] D. H. Bromwich al., *Nature Geoscience*, **6**, 139 (2012).
- [47] IPCC, Stocker T. F. et al. Eds. (2013), *Climate Change 2013: The Physical Science Basis. Contribution of Working Group I to the Fifth Assessment Report of the Intergovernmental Panel on Climate Change*, Cambridge University Press, Cambridge and New York.
- [48] J. W. Kantelhardt, E. Koscielny-Bunde, H.H.A. Rego, A. Bunde, and S. Havlin, *Physica A*, **295**, 441 (2001).
- [49] D. H. Bromwich et al, *Nature Geoscience*, **7**, 11247 (2014).
- [50] D. H. Bromwich and J. P. Nicolas, *Nature Geoscience*, **7**, 247 (2014).
- [51] T. Schreiber and A. Schmitz, *Phys. Rev. E*, **77**, 635 (1996).